OPTIMIZATION OF BIKE FRAME GEOMETRY AND TUBE SIZES FOR USA TRIATHLON EVENTS

Jacob Hartzer [1] and Jorge Montanez Aguilar [1]
[1] Texas A&M University, College Station, Texas, United States

1. INTRODUCTION

A triathlon is one of the few sports that depends on the quality and performance of a device to achieve optimal performance in a competition. The USA Triathlon Association (USAT) has registered more than 200,000 athletes with an annual membership (USAT, 2015), which represents around 35% of the total athletes present in the USAT events each year, this number keeps growing due to this sport is also taken as a personal challenge not just as a lifestyle.

The number of athletes for one-day registration for competition in the USAT goes from 299,030 (USAT, 2015) until 371,988 (USAT, 2011), from 2010 through 2015 demographic registration. The cost for a triathlon bicycle could be from 2000 USD until 15000 USD, where the main differences are weight, frame shape, material, and aerodynamic properties that also have to be within the USAT rules.

The triathlon bicycles that are currently in the market have an average weight of 8 kg (17.5 kg), where the frame represents an average of 1.36 kg (3 lb.) and the primary materials used for bicycle frames are AISI 1060 High Carbon Steel, ASTM A182 Chromoly Steel, Aluminum 6061-T4, Titanium, and Carbon Fiber.

This article analyses the stresses, moments and torques present in an over-constrained frame system and optimizes the design of a customized bicycle frame for triathlon competition using Matlab optimization toolbox to obtain the optimal geometry configuration and material selection and Solidworks to analyze the integrity of the frame based on the Matlab results.

2. PROBLEM FORMULATION

Bicycle frames used in USA triathlons are instrumental to the success of athletes. Weight reductions of the frame would increase the competitiveness of an individual athlete.

2.1 Objective

To create a bicycle frame that is capable of supporting the stresses of a rider seen in competition, conform to the rules of USA Triathlons, all while minimizing the material weight of the frame. To achieve this objective, the geometry and material of the frame will be adjusted, as well as the width, thickness, and aspect ratio of each tube. To simplify the problem, the model was broken up into 5 modules. These were: Geometry, Section Modulus, Stress, Rules, and Cost/Mass.

The objectives can be defined as follows:

$$\begin{bmatrix} J_1 \\ J_2 \end{bmatrix} = \begin{bmatrix} Frame\ Weight \\ Seat\ Height \end{bmatrix} \tag{1}$$

The objective functions can be defined as:

$$min(J_1(x)) \tag{2}$$

$$max(J_2(x)) \tag{3}$$

$$\mathrm{x} = \begin{bmatrix} Wheelbase \\ Handlebar_x \\ Handlebar_y \\ Pedal_x \\ Pedal_y \\ Seat_x \\ Seat_y \\ d \\ p \\ w(1) \\ \dots \\ w(7) \\ a(1) \\ \dots \\ a(7) \\ t(1) \\ \dots \\ t(7) \\ Material \end{bmatrix}$$

where:

2.1 N^2 Diagram

In order to organize the problem an N^2 diagram was created as shown in *Figure 1*. This diagram shows there is no coupling between any of the modules and the system is entirely feedforward, which aids computation time.

Inputs	Nodes		Mat'l	.	Mat'l.	Mat'l.
	Geom.		Geom.	Geom.	Geom.	Geom.
		Section Modulus	S			
			Stress			Stresses
				Rules		Stress
					Cost, Mass	Cost, Mass
						Output

Figure 1. N^2 Diagram

3. GEOMETRY MODEL

3.1 Method

In order to reduce the number of design variables without reducing the degrees of freedom of the algorithm, the geometrical design variables were defined as the intersection points of the tubes, rather than the lengths and positions of all tubes. This reduced the number of constraint equations, but also required a module for determining the geometry of the bicycle given the input vector.

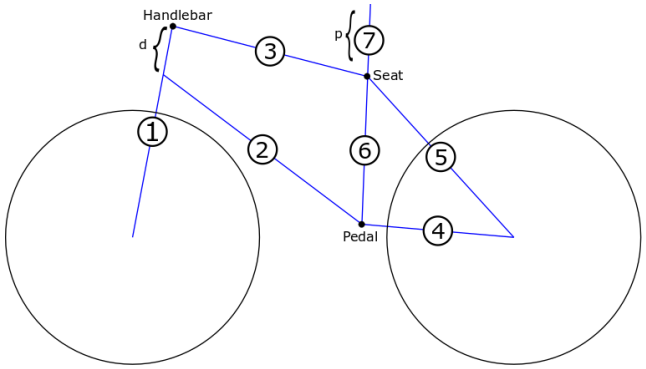

Figure 2. Input Variable Geometric Interpretation

The geometric module takes in the design vector in the form of node positions and lengths *d* and *p*, and outputs the lengths of each tube as well as the starting and ending position of each tube. This is done using by assuming the position of the front wheel and linearly extrapolating tube positions. While technically this information over defines the system, it proves useful in later calculations.

3.2 Constraints and Bounds

The geometrical model is constrained by the locations of tube 2 and tube 6 because these tubes cannot intersect with the wheels. As such, the following circle-line intersection equations are defined where it is assumed the circle lies at the origin and r is the wheel diameter plus the width of the tube times its aspect ratio.

$$d_x = x_2 - x_1 \tag{4}$$

$$d_y = y_2 - y_1 \tag{5}$$

$$d_r = \sqrt{d_x^2 + d_y^2} \tag{6}$$

$$D = \begin{vmatrix} x_1 & x_2 \\ y_1 & y_1 \end{vmatrix} = x_1 y_2 - x_2 y_1 \tag{7}$$

$$r^2 d_r^2 - D^2 < 0 \tag{8}$$

The bounds were set as:

$$800 < Wheelbase < 1300 \tag{9}$$

$$350 < Handlebar_x < 550 \tag{10}$$

$$600 < Handlebar_y < 1000 \tag{11}$$

$$700 < Pedal_x < 1300 \tag{12}$$

$$240 < Pedal_y < 400 \tag{13}$$

$$400 < Seat_x < 1500 \tag{14}$$

$$500 < Seat_y < 1000 \tag{15}$$

$$0 < d < 250 \tag{16}$$

$$1 < p < 400 \tag{17}$$

4. SECTION MODULUS MODEL

4.1 Method

In order to simplify the solving of the stress model, the section modulus is found for each tube. The modulus relates the applied moment to the maximum stress of tubes of a particular shape. Because the model assumes the tubes to have a hollow oval shape, as shown in *Figure 3*, knowing the section modulus simplifies the internal stress calculation in the following module. In the following diagram, *b* is the tube width.

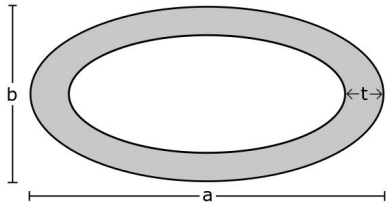

Figure 3. Tubular Cross-Sectional Shape

$$Aspect\ Ratio = \frac{b}{a} \tag{18}$$

$$S = \frac{\pi(ab^3 - (a-t)(b-t)^3)}{32a} \tag{19}$$

4.2 Constraints and Bounds

The section modulus module is constrained in that the thickness of the tube cannot be greater than half the width of the tube width. Additionally, because the tube 7 is to fit within tube 6, the outer perimeter of tube 7 cannot intersect the inner perimeter of tube 6.

$$2t \leq w \tag{20}$$

$$w(7) \leq w(6) - 2t(6) \tag{21}$$

The bounds were set as:

$$1 < aspect < 5 \tag{22}$$

$$0.001 < thickness < 25 \tag{23}$$

$$1 < width < 100 \tag{24}$$

5. STRESS MODEL

5.1 Method

The stress model makes use of the previous two modules to determine the internal moments and reaction forces experienced by the tubes. In order to determine these forces and moments, the frame problem was converted to seven beam problems, with the nodes and forces defined in *Figure 4*.

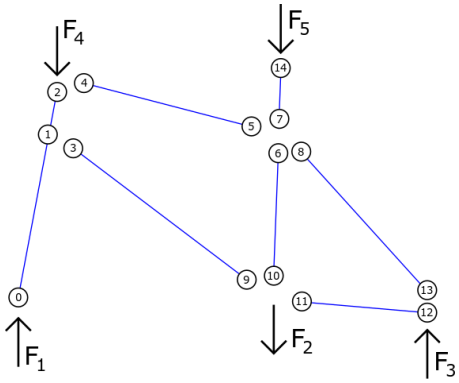

Figure 4. Frame Loadings and Node Numbers

With the loadings defined and reaction forces and moments placed at each node, force and moment balance equations were written for each beam and node. This provided 24 force or moment balance equations for a total of 26 unknown variables. The extra two variables are due to the overconstrained nature of the bicycle frame, whereby two of the interior members (for example tube 2 and 6) could be removed to become a statically determinate problem. In order to overcome the missing two equations, the direct displacement method was applied. In this method, a rotational displacement was applied to the pedal sprocket in order to determine the reactionary moments experienced by the tubes. This displacement is exemplified in *Figure 5*.

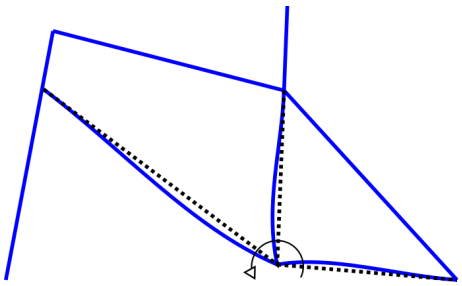

Figure 5. Direct Displacement Applied Rotation

From this displacement, the following relationship could be found between the properties of the tube and the internal moment:

$$\frac{E_2 M_2 S_2 a_2 w_2}{L_2} = \frac{E_6 M_6 S_6 a_6 w_6}{L_6} \tag{25}$$

This equation can be used to supplant one of the missing equations. Applying this method to the top tube intersection supplies the second missing equation.

With these additional equations, the system can be solved as a 26x26 matrix with the applied forces as a solution vector. Solving the matrix equation provides the internal moments and reactionary forces experienced by the tubes.

5.2 Constraints and Bounds

The constraints formed from the internal stresses arise from the material limits of the tubes. The internal stress can be calculated as a combination of the axial and bending stresses experienced by the tubes. This stress must therefore be kept below the failure stress of the selected material.

$$\sigma = \frac{My}{I} + \frac{P}{A} = \frac{M}{S} + \frac{P}{A} \tag{26}$$

$$\sigma \leq \sigma_f \tag{27}$$

5.3 Validation

The stress model was validated using a Solidworks model. After running a simple optimization script, the resultant geometries were used to create the solid model shown in *Figure 6.* Using identical loadings and material properties, the solidworks model showed the same margin of safety that the stress module predicted. As such, there is high confidence in the accuracy of the stress model.

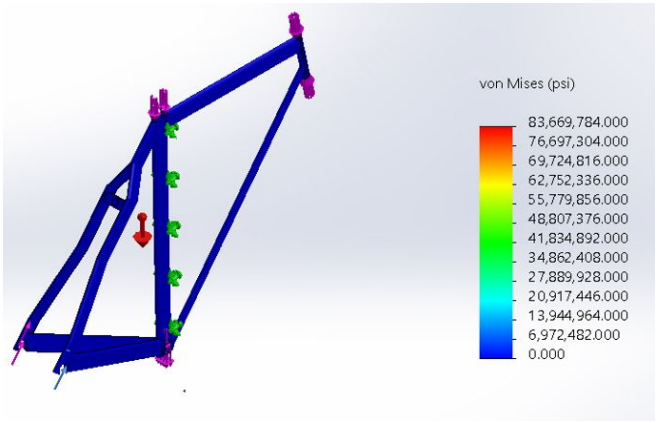

Figure 6. SolidWorks Simulation

6. USA TRIATHLON RULES

Because of the nature of this problem, there are also constraints that arise not from physical limits, but the rules set forth by the governing body of USA Triathlons.

6.1 Constraints and Bounds

The USA Triathlon rules mainly pertain to the allowable geometries of the bicycle. The relevant geometrical constraints are shown in the following equations.

$$Length \leq 2m \tag{28}$$

$$-5cm \leq Seat_x - Pedal_x \leq 15cm \tag{29}$$

$$Pedal_y \geq 24cm \tag{30}$$

$$54cm \leq Pedal_x - \frac{WheelDiameter}{2} \leq 65cm \tag{31}$$

7. OBJECTIVE FUNCTION CALCULATION

The overall mass of the frame is one of the objection functions. In order to calculate the mass, the lengths as calculated by the geometrical module is multiplied times the material density and calculated cross-sectional areas. Moreover, the cost of the material, if desired, can be calculated by multiplying the mass times the cost density of the material. These equations are shown below.

$$Mass = \sum \rho\pi\mathbf{L} \cdot \left(\frac{\mathbf{a} \cdot \mathbf{w}^2}{4} - \frac{\mathbf{a} \cdot (\mathbf{w} - 2\mathbf{t})}{2} \cdot \frac{\mathbf{w} - 2\mathbf{t}}{2} \right) \tag{32}$$

$$Cost = \sum C_m\rho\pi\mathbf{L} \cdot \left(\frac{\mathbf{a} \cdot \mathbf{w}^2}{4} - \frac{\mathbf{a} \cdot (\mathbf{w} - 2\mathbf{t})}{2} \cdot \frac{\mathbf{w} - 2\mathbf{t}}{2} \right) \tag{33}$$

Additionally, the seat height can be calculated by summing the lengths of tubes 6 and 7.

$$Seat\ Height = L(6) + L(7) \tag{34}$$

8. DESIGN SPACE EXPLORATION

In order to explore the design space, an initial design vector was defined by using an existing design of a commuter-style bicycle. This design was checked and shown to be feasible within the model. With this design as the base case, a OVAT experiment was designed with 40 levels for each of the 30 continuous design variables and 5 levels for the integer material variable. This process resulted in 1175 experiments, with 664 being feasible and the current minimal weight being 4.0581 kg. The largest effects were seen from changing the wheelbase and thickness and aspect ratio of the longest tube (2). Generally, reducing the width, aspect ratio, and thickness result in lighter frames, but that have higher internal stresses. This is the main crux of the problem, and the justification for optimization.

9. ALGORITHM SELECTION

9.1 Gradient Method

This problem as defined has a large number of nonlinear constraints. Additionally, the design space seems very complex. As such, SQP seems like a great option for handling these nonlinearities while still being able to traverse the design space.

For the sake of single objective optimization of this system, frame weight was chosen. This is because the weight of the frame is generally seen as correlated with speed of triathlon bikes and lighter frames require less power during hill climbs. The seat height objective will be ignored for now.

Implementation of SQP from the feasible solutions of the DOE resulted in convergence in every case and satisfaction of constraints within 1e-8. Thirty seven of the solutions, including the best solution found resulted in true satisfaction of constraints. From the ten solutions checked, the active constraint was always from the internal stress of the tubes. In every case an improvement of 50% or more was seen.

From this work, the optimal solution was found at a weight of 0.414 kg. An generated image of the frame can be seen in *Figure 7*.

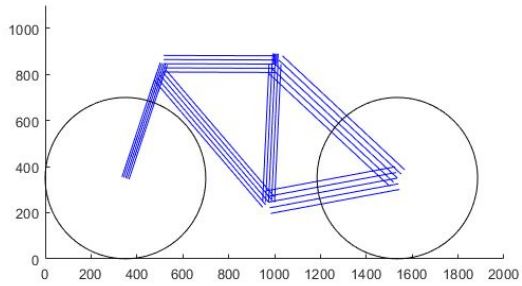

Figure 7. SQP Optimal Solution

9.1 Heuristic Method

A genetic algorithm was chosen because of the integer variables for the tube material. A GA would very naturally be able to handle this, and therefore it seemed like the best choice for a Heuristic algorithm implementation.

Initially trying to solve the problem with a GA was not met with much success. It took a large number of generations before the solutions approached a reasonable value.

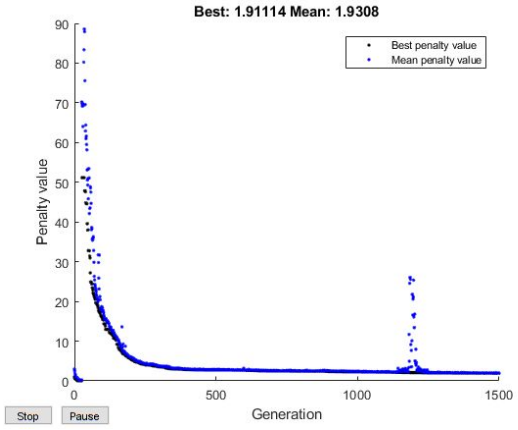

Figure 8. Original GA convergence

Attempting to tune the parameters led to slight improvements in speed and convergence, but not to the point that was seen from a gradient method. The found parameters that worked best were Pop = 50, MaxGen = 500, Elites = 1, Crossover Fraction = 0.5, Constraint Tol = 1e-8, Max Stall Gen = 100.

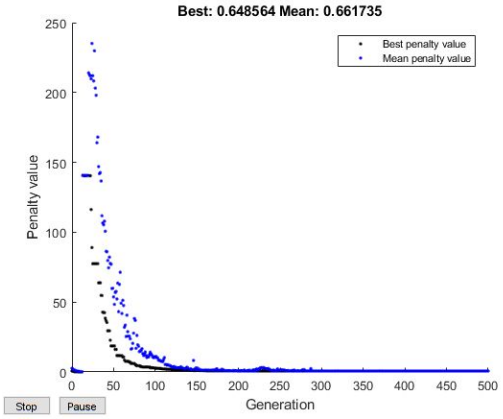

Figure 9. Tuned GA convergence

Despite the tuning efforts, the genetic algorithm was never able to reach values as low as those seen by the gradient method. Therefore, despite being able to give good results, SQP with multistart is deemed most appropriate for solving this problem.

10. SENSITIVITY ANALYSIS

The sensitivity analysis has been performed at the optimal point found by the multistart SQP algorithm previously discussed. The sensitivity of the weight of the frame is shown through the computation of the gradient for the entire design vector. Additionally, the normalized gradient is shown. What can been determined from the normalized gradient is changing the wheelbase has the largest relative impact on the weight of the frame. Additionally, the widths and thicknesses of the tubes have medium-order effects.

Moreover, sensitivity about certain parameters was also performed. Shown are the sensitivities the design variables have to the stress limit and applied force parameters. What can be gathered here is that deviations in the maximum stress limit have very large impacts on the design variables, especially when compared to deviations in the applied force (rider weight). The variables most affected by the material properties were the tube thicknesses and widths, whereas the handlebar location was most affected by the change in the applied force.

$$J = \begin{bmatrix} 5.00E-04 \\ -3.00E-04 \\ 2.00E-04 \\ -2.00E-04 \\ -3.00E-04 \\ 1.00E-04 \\ 2.00E-04 \\ -1.00E-04 \\ 0.00E+00 \\ 3.54E-02 \\ 1.86E-01 \\ 1.03E-01 \\ 1.92E-01 \\ 5.37E-02 \\ 5.68E-02 \\ 2.00E-03 \\ 1.41E-01 \\ 2.08E-01 \\ 1.39E-01 \\ 1.67E-01 \\ 5.49E-01 \\ 1.69E-01 \\ 8.00E-03 \\ 7.00E-04 \\ 3.70E-03 \\ 2.00E-03 \\ 3.60E-03 \\ 2.70E-03 \\ 1.10E-03 \\ 1.00E-04 \end{bmatrix} \qquad \bar{J} = \begin{bmatrix} 1.32E+00 \\ -4.13E-01 \\ 5.03E-01 \\ -3.84E-01 \\ -2.03E-01 \\ 1.74E-01 \\ 4.45E-01 \\ -1.60E-02 \\ 4.00E-03 \\ 8.60E-02 \\ 4.48E-01 \\ 2.48E-01 \\ 4.63E-01 \\ 1.30E-01 \\ 1.37E-01 \\ 5.00E-03 \\ 8.50E-02 \\ 1.33E-01 \\ 8.40E-02 \\ 1.60E-01 \\ 3.31E-01 \\ 1.02E-01 \\ 5.00E-03 \\ 5.60E-02 \\ 6.00E-01 \\ 3.55E-01 \\ 8.79E-01 \\ 6.22E-01 \\ 1.43E-01 \\ 4.00E-03 \end{bmatrix} \tag{35}$$

$$\frac{\partial x}{\partial \sigma} = \begin{bmatrix} 7.11E-01 \\ -1.07E+00 \\ 2.69E-01 \\ 7.87E-01 \\ -4.08E-01 \\ -2.99E-01 \\ 3.23E-01 \\ -1.29E-01 \\ 3.68E-01 \\ 0.00E+00 \\ 0.00E+00 \\ 0.00E+00 \\ 0.00E+00 \\ -1.58E+00 \\ 0.00E+00 \\ 0.00E+00 \\ 4.80E+00 \\ 4.17E+00 \\ 4.31E+00 \\ 3.92E+00 \\ 4.80E+00 \\ 4.71E+00 \\ 3.79E+00 \\ 1.22E+00 \\ -1.66E+00 \\ -1.24E+00 \\ -3.77E+00 \\ -2.01E+00 \\ -1.83E-01 \\ 6.66E-01 \end{bmatrix} \qquad \frac{\partial x}{\partial F} = \begin{bmatrix} -1.89E+00 \\ 3.29E+00 \\ -6.28E-01 \\ -2.42E+00 \\ 1.02E+00 \\ 7.01E-01 \\ -7.32E-01 \\ 3.62E-01 \\ -7.63E-01 \\ 5.45E-03 \\ 0.00E+00 \\ 4.23E-02 \\ 4.65E-05 \\ -6.91E-01 \\ 7.31E-02 \\ 0.00E+00 \\ 0.00E+00 \\ -2.29E-01 \\ -1.59E-01 \\ -4.07E-01 \\ 2.16E-03 \\ 9.77E-02 \\ 0.00E+00 \\ -1.91E+00 \\ 8.18E+00 \\ 5.74E+00 \\ 1.23E+01 \\ 6.33E+00 \\ 2.28E+00 \\ -1.34E+00 \end{bmatrix} \tag{36}$$

11. SCALING

The diagonal elements of the Hessian with the associated scalings are shown below in *Equation 37*:

After application of scaling, the solutions converged on much lower frame weights at a much more consistent rate with 23 of the runs getting within 0.01 kg of the minimal value. This minimal value was 0.2039 kg.

$$diag(H) = \begin{bmatrix} -2.62E-09 \\ 2.72E-09 \\ -1.35E-09 \\ 1.55E-09 \\ 7.50E-09 \\ -5.86E-11 \\ -1.92E-09 \\ 9.67E-09 \\ -6.81E-09 \\ -2.28E-04 \\ -7.14E-04 \\ -4.79E-04 \\ -1.23E-03 \\ -9.58E-04 \\ -4.26E-04 \\ -1.42E-05 \\ -3.62E-03 \\ -1.02E-02 \\ -7.63E-03 \\ -7.84E-03 \\ -1.54E-02 \\ -6.71E-03 \\ -2.25E-04 \\ -2.24E-07 \\ -1.55E-07 \\ -9.20E-08 \\ -1.24E-07 \\ -1.03E-07 \\ -1.59E-07 \\ -2.73E-08 \end{bmatrix} \quad 10E \begin{bmatrix} -5 \\ -5 \\ -5 \\ -5 \\ -5 \\ -6 \\ -5 \\ -5 \\ -5 \\ -2 \\ -2 \\ -2 \\ -2 \\ -2 \\ -2 \\ -3 \\ -2 \\ -1 \\ -2 \\ -2 \\ -1 \\ -2 \\ -2 \\ -4 \\ -4 \\ -4 \\ -4 \\ -4 \\ -4 \\ -4 \end{bmatrix} \tag{37}$$

12. FINAL DESIGN

The chosen final solution is shown in *Figure 10* and *Equation 38* lists the selected variables.

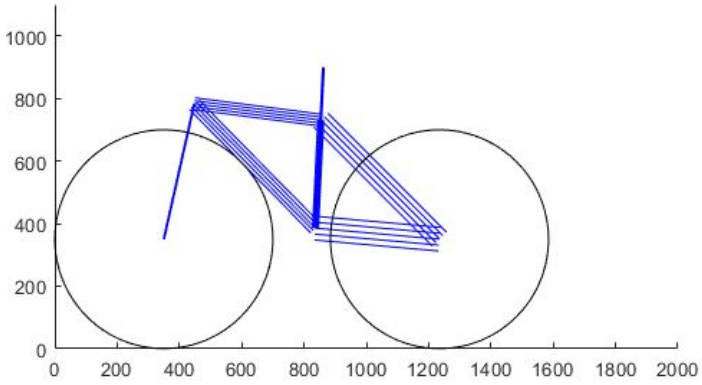

Figure 10. Final Frame Design

$$x = \begin{bmatrix} 8.85E-03 \\ 4.48E-03 \\ 7.83E-03 \\ 8.37E-03 \\ 3.85E-03 \\ 8.54E-04 \\ 7.31E-03 \\ 3.01E-05 \\ 1.69E-03 \\ 1.00E-02 \\ 1.00E-02 \\ 1.00E-02 \\ 1.00E-02 \\ 1.01E-02 \\ 1.08E-02 \\ 3.29E-03 \\ 5.61E-03 \\ 5.96E-02 \\ 8.39E-03 \\ 6.01E-03 \\ 5.66E-02 \\ 6.81E-03 \\ 1.03E-02 \\ 3.43E-04 \\ 4.27E-03 \\ 3.79E-03 \\ 7.59E-03 \\ 6.31E-03 \\ 1.87E-03 \\ 5.28E-04 \\ 5.00E+00 \end{bmatrix} \tag{38}$$

The final mass of this design is 0.4013 kg.

13. POST OPTIMALITY ANALYSIS

In addition to the sensitivity analysis performed, a pareto front was found around the selected design vector. Shown in *Figure 11*, the pareto front shows the negative of seat height with respect to frame weight. The estimated pareto front has a natural corner that also falls well within the required inseam range of most athletes while also maintaining an extremely low frame weight. Therefore, the point shown in red was the selected final solution.

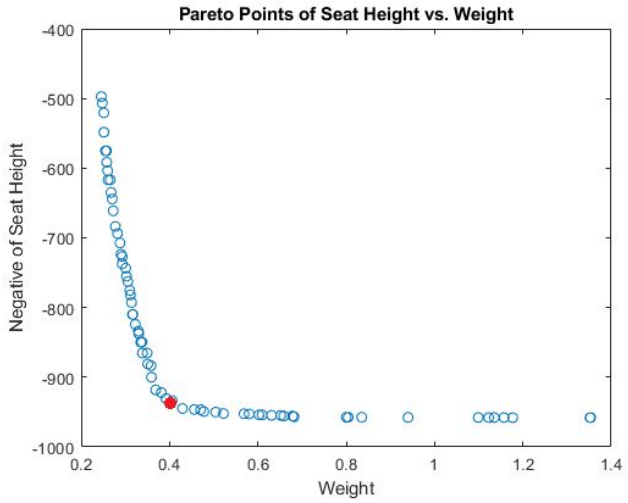

Figure 11. Estimate of Pareto Front

14. CONCLUSIONS

Using a tuned GA was inconsistent in finding a solution to the problem. However, using a well scaled problem definition and thorough multi-start testing, we are quite confident in the global optimality of the solution found through SQP. This solution serves as an excellent balance between weight and seat height, and the results of this analysis will give riders the information needed to select the best frame for themselves.

REFERENCES

Automation Creations, Inc. *MatWeb, Your Source for Materials Information*. 2019

Budynas, Richard and J. Keith Nisbett. *Shigley's Mechanical Engineering Design.* 2015

Fanous, Fouad. *Direct Displacement Method: Indeterminate Frame*, 2019

USA Triathlon. *Competitive Rules.* 2019